

# Predicting graded dishabituation via perceptual stimulus embeddings in a rational learning model

Anonymous CogSci submission

## Abstract

How do humans decide what to look at and when to stop looking? The Rational action, noisy choice for Habituation (RANCH) model formulates looking behaviors as a rational information acquisition process. RANCH instantiates a hypothesis about the perceptual encoding process through neural network-derived embedding space, allowing it to operate on raw images. In this paper, we show that the model not only captures key looking time patterns such as habituation and dishabituation, but also makes fine-grained, out-of-sample predictions about magnitudes of dishabituation to previously unseen stimuli. We validate those predictions experimentally with a self-paced looking time task in adults ( $N = 468$ ). We also show that the model is robust across parameters, but the assumptions about the perceptual encoding process, the learning process and the decision process are all critical for the model performance.

**Keywords:** Add your choice of indexing terms or keywords; kindly use a semi-colon; between each term.

## Introduction

From birth, humans learn actively. Even before they can move on their own, infants can select information by deciding what to look at and when to stop looking (Haith, 1980; Raz & Saxe, 2020). Developmental psychologists have long leveraged this attentional decision-making to make inferences about the perceptual and cognitive abilities of infants by measuring how long infants look at certain stimuli (Aslin, 2007; Baillargeon, Spelke, & Wasserman, 1985; Fantz, 1963).

Two key phenomena are particularly critical for these inferences: habituation and dishabituation. Habituation refers to the decrease in looking time upon seeing the same or similar stimuli repeatedly; dishabituation refers to the increase in looking time following the presentation of a novel stimulus after habituation. In order to dishabituate, the infant must distinguish between the original stimulus and the novel one. While habituation and dishabituation have been robustly documented, the underlying mechanisms of these looking time changes remain poorly understood. In this paper, we address this gap by presenting a rational model that provides principled predictions on the magnitude of dishabituation. Critically, this model can be applied generally to make predictions about looking time for arbitrary stimuli by using embeddings derived from a convolutional neural network.

The dominant framework in explaining changes in looking time proposes that habituation and dishabituation are driven by the amount of information to be encoded in the stimulus

(Hunter & Ames, 1988). Observers look longer at a stimulus if the stimulus has a lot of unencoded information, and as exposure to the stimulus accumulates, less information is left unencoded, leading to shorter looking time. While this theory has been highly influential, the lack of formal details about what is meant by “encoding” opens the door for post-hoc interpretation of looking time measurements. A stimulus could be argued to be novel because it has distinct perceptual features, but it could also be familiar because of its conceptual characteristics. In part as a result of this interpretive ambiguity, concerns have been raised about whether looking time measurements should be the foundation for central claims in developmental psychology (Blumberg & Adolph, 2023; Haith, 1998; Paulus, 2022).

Computational models provide an important tool for formalizing the details of the habituation and dishabituation process. One set of models describes infants’ looking behaviors with information-theoretic measures derived from ideal observer models (Kidd, Piantadosi, & Aslin, 2012; Francesco Poli, Ghilardi, Mars, Hinne, & Hunnius, 2023; F. Poli, Serino, Mars, & Hunnius, 2020). For example, Francesco Poli et al. (2023) developed a model that calculates the Kullback–Leibler (KL) divergence of each event infants saw in an experiment. This measure was shown to predict infants’ looking time, with higher KL associated with to longer looking time.

While these models provided quantitative accounts of the habituation process, they do not model the infant’s information sampling process directly. Instead, they describe trial-level correlations between these information-theoretic measures and measured looking times. In other words, these models do not explain how information theoretic measures are causally related to the sampling decision at any given moment. Furthermore, these prior models presuppose an abstracted representation of the stimuli, and do not instantiate a precise hypothesis about how visual encoding occurs during attentional decision-making. This limits the ability of these models to make principled predictions on new, unseen stimuli.

To address these issues, Rational Action, Noisy Choice for Habituation (RANCH) model was developed (Cao, Raz, Saxe, & Frank, 2023; Raz, Cao, Saxe, & Frank, 2023). RANCH describes an agent’s looking behavior as a rational exploration of noisy perceptual samples. This model construes the looking time paradigm as a series of binary de-

cisions: to keep sampling from the current stimulus, or to move on to the next stimulus. This model makes sampling decisions based on the Expected Information Gain (EIG) of the perceptual samples, and therefore can be seen as a rational analysis of looking behavior (Anderson, 1991; Lieder & Griffiths, 2020; Oaksford & Chater, 1994).

RANCH incorporates recent progress in convolutional neural networks, which have offered insights into how the visual system encodes objects (Doshi & Konkle, 2023; Hebart, Zheng, Pereira, & Baker, 2020; Yamins et al., 2014). The activations of these brain-inspired neural networks form embedding spaces, each of which can be seen as a quantitative hypothesis about how humans represent visual stimuli (Schrimpf et al., 2020). For example, Lee (2022) projected the final layer of a trained ResNet50 into a “perceptually-aligned” space, by making its representations match dissimilarity matrices derived from human adult reaction times in a 2-AFC match-to-sample task. Passing new stimuli through this perceptual alignment yields a plausible representation of how humans embed different visual stimuli in a low-dimensional space. Using this perceptually-aligned embedding space as a model of perceptual encoding, RANCH can generate fine-grained predictions about how long observers will look at previously unseen stimuli.

Previously, Cao et al. (2023) and Raz et al. (2023) have shown that RANCH can successfully model habituation and dishabituation in adults and infants. Here, we test RANCH’s ability to (1) predict responses in new data, and (2) predict a key phenomenon in qualitative accounts of habituation. For the first test, we tune its parameters to behavior on a generic habituation and dishabituation task, and test its performance on a previously unseen behavioral dataset. For the second test, we focus on RANCH’s ability to reproduce a prediction from Hunter & Ames (1988) model of habituation and dishabituation: that observers’ dishabituation magnitude should be related to the similarity between the habituated stimulus and the novel stimulus. The more dissimilar two stimuli are, the more one should dishabituate to the novel stimulus.

To conduct these tests, we first fit RANCH’s parameters to the training data, a dataset from the habituation-dishabituation experiment in which participants saw sequences of monsters which were either familiar or novel (dataset reported in Cao et al., 2023, Fig 1A). Then, we use the best-fitting parameters to generate predictions for a new experiment that measure the subtle differences in dishabituation magnitude based on stimulus similarity (Fig 1C). In this experiment, we systematically varied the similarity between habituation and dishabituation stimuli such that dishabituation stimuli differed in their pose angle, their number, their identity, or their animacy.

To preview our results, we show that RANCH can predict looking time responses in new data just by transferring model parameters fit from previous data, with marginal differences in performance compared to completely refitting to the new data. RANCH also captured the particular ordering

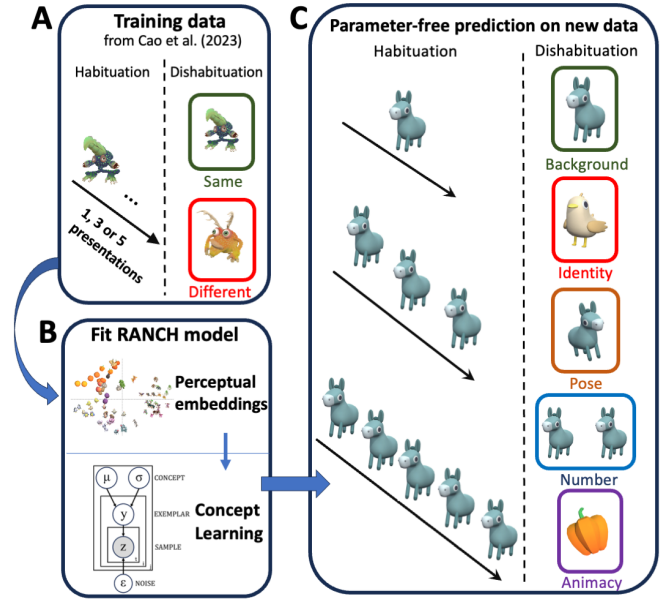


Figure 1: Workflow of the current study. (A) The experimental design and stimuli used in the training dataset. (B) The core components of RANCH, with the top showing the stimuli embedding in PC-space. The bottom is the plate diagram of the learning model. (C) The experimental design of the test data. RANCH model is first fit using the training data in A, and we test its prediction on the test data collected in the experiment illustrated in C.

of the dishabituation magnitude as a function of stimulus dissimilarity, thereby predicting a novel qualitative phenomenon (graded dishabituation) without ever being trained on it. Finally, we show that RANCH is relatively robust across parameter settings, but the assumptions about its perceptual representation, learning process, and the decision process are all critical to its performance.

## Model

### Model Components

We modeled looking behaviors in our task as rational information acquisition, using a “rational analysis” approach previously described for different information-seeking behaviors (Dubey & Griffiths, 2020; Oaksford & Chater, 1994). Our goal was to develop a model which formalizes the entire process underlying looking time: from perception of a stimulus to deciding how long to look at it. To do so, our model has three separate components describing (1) how stimuli are embedded a low-dimensional perceptual space (2) how RANCH learns a concept over this perceptual space and (3) how RANCH makes decisions about how long to sample from a stimulus based on its expected information gain. Here, we describe these three components in turn.

**Perceptual representation** To allow RANCH to operate on raw images, we used the perceptually-aligned embeddings obtained from a model presented recently by Lee (2022). We use these projections into a perceptually-aligned embedding space as a principled low-dimensional representation of stimuli, over which our learning model can form perceptual concepts. We used the first three principal components of the embedding space, which captured 57.9% of the variance. A visualization of experimental stimuli in the embedding space can be seen in Figure 1B.

**Learning model** RANCH’s goal is to learn a concept in the perceptual embedding space described above, through noisy perceptual samples from a stimulus. The concept is parameterized by a 3D Gaussian  $(\mu, \sigma)$ , which represents beliefs about the location and variance of the concept in the embedding space. This concept  $(\mu, \sigma)$  generates exemplars ( $y$ ): exemplars of the concept. RANCH observes repeated noisy samples ( $\tilde{z}$ ) from each exemplar. For any sample ( $z$ ) from an exemplar ( $y$ ), the model expects the observation to get corrupted by zero-mean gaussian noise with standard deviation ( $\epsilon$ ). A plate diagram is shown in Figure 1B. We used a normal-inverse-gamma prior on the concept, the conjugate prior for a normal with unknown mean and variance, on the concept parameterized as  $\mu_p, \nu_p, \alpha_p, \beta_p$ . Still, applying perceptual noise to  $y$  breaks the conjugate relation, so we computed approximate posteriors using grid approximation over  $(\mu, \sigma)$  and  $(\epsilon)$ . This computationally expensive approximation was accomplished through a PyTorch implementation and distributed GPU computation.

**Decision model** To decide whether to take an additional sample from the same stimulus, RANCH computes expected Information Gain (EIG) of the next sample. EIG is computed as the product of the posterior predictive probability of the next sample and the information gained conditioned on that next sample, by iterating through a grid of possible subsequent samples. RANCH then makes a softmax choice (with temperature = 1) between taking another sample and looking away. We assumed that participants expect a constant information gain from looking away (the “world EIG”). Therefore, as EIG from the stimulus drops below world EIG, it becomes increasingly likely that RANCH will look away.

## Alternative models

To test the importance of each of RANCH’s components for its performance, we defined three lesioned models, in which one key feature of the model was removed. First, to test the importance of the perceptual embeddings, we ran a version of RANCH in which the mappings from stimulus labels to embeddings were permuted, such that the associations between embeddings and violation type were randomized (“Random embeddings”). Second, we ran a version in which RANCH assumes that each perceptual sample in the learning process is noiseless, rather than corrupted by  $\epsilon$  (“No noise”). Third, we ran a version in which RANCH made decisions randomly

rather than based on the learning model (“No learning”).

## Training Procedure

We used the behavioral dataset reported in Cao et al. (2023) as the training data. In this prior experiment, 449 adults participated in an online self-paced looking time paradigm (Fig. 1A). In this paradigm, participants watched blocks of six animated monsters. Each block consisted of one repeating monster (the background), and one monster different from the repeated one (the deviant). The deviant, if shown, was on either the 2nd, 4th, or 6th trial of the block. Adults can proceed to the next trial whenever they press a key on the keyboard, and the interval between the onset of the stimuli and the key press was used as the proxy for looking time. To train on this dataset, we first converted the raw stimuli into perceptual embeddings, and combined them into stimuli sequences identical to the sequence participants have seen. Since the model makes stochastic sampling decisions, we conducted 400 runs for each stimuli sequence for each parameter setting. To avoid numerical instabilities due to the granularity of our grid approximation, for each run we slightly jittered all parameter grid values by a constant offset. We conducted an iterative grid search across the priors over  $\mu$ ,  $\nu$  and  $\epsilon$ , along with the actual noise  $\epsilon$ . We selected the parameters that yielded the highest  $R^2$  between the model output and the behavioral data as the best fitting parameters. The best fitting parameters were ( $\mu_p = 0, \nu_p = 1, \alpha_p = 1, \beta_p = 1, \epsilon = 0.0001$ ).

## Behavioral Experiment

Next, we introduce the novel experiment used to test the generalizability of the parameter setting found above. The procedure was similar to the previous training data with two key differences: First, stimuli used in this previous experiment were animated monsters, but the current experiment used images of animals and vegetables with added shaking animations. Second, unlike the previous experiment, the current study manipulated the dissimilarity between the repeating stimulus and the deviant stimulus by introducing different types of deviant stimuli.

## Methods

**Stimuli** All stimuli were created using images selected from Unity assets “Quirky Series - Animals” and “3D Prop Vegetables and Fruits”. We added the same minor shaking animation to each image to increase interest. For each image from the animal set, we created a mirrored version to create an image with a different pose. Since most stimuli from the vegetable set were symmetrical, the images were slightly tilted before mirroring.

**Procedure** The experiment was a self-paced web-based experiment (Fig. 1C). Participants saw 24 blocks that consisted of either two, four, or six trials. On each trial, a schematic screen would rise up to reveal a stimulus behind it. Participants pressed the spacebar to go on to the next trial after a minimum viewing time of 500 ms, triggering the schematic

screen to drop and raise again to reveal the next stimulus.

Each participant saw eight types of repeating stimuli. The eight types of stimuli included all combinations of the three features that each included two levels: animacy (e.g. animate or inanimate), number (singleton or pair), and pose (facing left or right).

Eight blocks consisted of one stimulus being repeatedly presented throughout the block (background blocks). The remaining sixteen blocks included two stimuli, including one that was repeatedly present and one that deviated from the repeating trial. The deviant trial was always different from the repeating stimulus in one of the four dimensions: animacy, identity, number, and pose. The deviant trial always showed up in the last trial of the block. In the first three violation types, the feature would be switched to the previously unseen level (e.g. an inanimate deviant after an animate repeating stimulus, keeping the number and the pose the same). For identity violations, the participants would see a different, but within-category, exemplar from the repeating stimuli type. Among the sixteen blocks, the four violation types each appeared four times. After each block, participants performed a simple memory task as a filler task.

To control the distribution of background blocks and deviant blocks, we grouped the 24 blocks into four groups. Each group consisted of two background blocks, and one deviant block from each violation type. The order of blocks within each group was randomized.

**Participants** We recruited 550 adult participants on Prolific. Participants were excluded if either (1) the standard deviation of log-transformed of their reaction times on all trials was less than 0.15 (indicating key-smashing); (2) they spent more than three absolute deviations above the median of the task completion time as reported by Prolific, or (3) they provided the incorrect response to more than 20% of the memory task. After the participant-level exclusion, we also applied trial-level exclusion. A trial was excluded from final analysis if it was three absolute deviations away from the median in the log-transformed space across all participants. The final sample included 468 participants.

## Results

The sample size and analysis plan were all pre-registered and can be found here. All analysis scripts are publicly available and can be found here [LINK].

We were primarily interested in (1) whether our experimental paradigm captured habituation and dishabituation and (2) whether the magnitude of dishabituation was influenced by the type of violation. We tested these two hypotheses in a linear mixed-effect model with maximal random effect structure that predicted log-transformed looking time with the following specification on the fixed effect:  $\log(\text{total\_rt}) \sim \text{trial\_number} + \text{is\_first\_trial} + (\text{trial\_number} + \text{is\_first\_trial}) * \text{stimulus\_number} + (\text{trial\_number} + \text{is\_first\_trial}) * \text{stimulus\_pose} + (\text{trial\_number} + \text{is\_first\_trial}) * \text{stimulus\_animacy} +$

$(\text{trial\_number} + \text{is\_first\_trial}) * \text{violation\_type} + \log(\text{block\_number})$ . The `violation_type` has five levels, including the background trial and four types of violation.<sup>1</sup>

Through different parameterization of the model (i.e. setting different baseline levels for violation type), we found evidence for habituation and graded dishabituation (Fig. 2). When the background test trial was treated as the baseline, there was a significant effect of trial number ( $\beta = -0.02$ ,  $SE = 0$ ,  $p < .001$ ). Moreover, looking time to animacy violations was significantly longer than to number violations ( $\beta = 0.17$ ,  $SE = 0.04$ ,  $p < .001$ ) and pose violations ( $\beta = 0.18$ ,  $SE = 0.04$ ,  $p < .001$ ), and so were identity violations (cf. number:  $\beta = 0.18$ ,  $SE = 0.04$ ,  $p < .001$ ; cf. pose:  $\beta = 0.19$ ,  $SE = 0.04$ ,  $p < .001$ ). But animacy violation was not different from the identity violation, nor was the number violation different from the pose violation (all  $p > 0.1$ ).

We also pre-registered a qualitative prediction on the ordering of the dishabituation magnitude (i.e. category  $>$  number  $>$  identity  $>$  pose). However, we did not find evidence consistent with this prediction. The qualitative ordering in our data was animacy ( $M = 2694.74$ ), identity ( $M = 2489.2$ ), pose ( $M = 2201.44$ ) and number ( $M = 2117.63$ ).

## Model Evaluation

### Parameter generalizability

The procedure to model the current experiment is very similar to the training procedure. We first converted the raw images into the perceptual representations. Then, we assembled the stimuli into sequences following the stimuli sequence participants saw in each block. For the block with deviating stimuli, we sampled deviant stimuli from corresponding violation categories. We sampled 23 stimuli pairs for each combination of violation type and deviant position.

However, instead of searching for a new set of best-fitting parameters, we used the best parameters found in the training dataset, and tested their generalizability to the new task. The best fitting parameters ( $\mu_p = 0$ ,  $v_p = 1$ ,  $\alpha_p = 1$ ,  $\beta_p = 1$ ,  $\epsilon = 0.0001$ ) predicted the habituation and dishabituation in the training data ( $R^2 = 0.95$  [0.90, 0.98]). Using these previously obtained parameters, we now test RANCH's performance on the current experiment with different stimuli and design. We found that the parameters generalized to the current context well ( $R^2: 0.75$  [0.68, 0.96],  $RMSE: 148.46$  [112.18, 219.54]). Moreover, RANCH also showed a qualitative ordering of the graded dishabituation similar to the behavioral data: animacy  $>$  identity  $>$  number  $>$  pose.

### Parameter robustness

To evaluate RANCH's robustness to different parameters, we then conducted a grid search over the parameters on the new experiment. We selected the best fitting parameters ( $\mu_p = 0$ ,  $v_p = 2$ ,  $\alpha_p = 10$ ,  $\beta_p = 1$ ,  $\epsilon = 0.0001$ ) using a 10-fold

<sup>1</sup>In our preregistered model, we specified an interaction between `trial_number` and `is_first_trial` that was automatically removed in the final model.

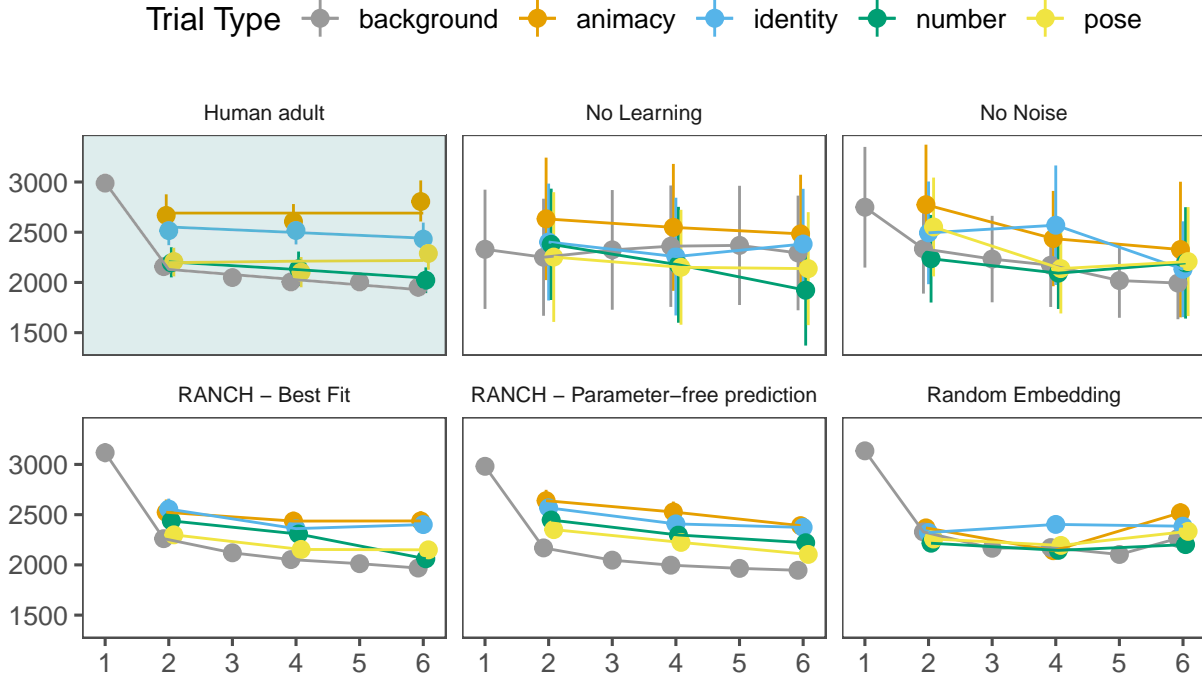


Figure 2: Human behaviors and model performance of RANCH and alternative models. For the human panel, X-axis shows the trial number, y-axis shows the looking time at each trial to the test stimuli in milliseconds. The line shows the fit from the preregistered linear mixed effect model. For the remaining panels, Y-axis represents the samples model made on each trial, scaled to the behavioral data. Different colors represents different trial types.

cross-validation on the behavioral dataset. When fit to the full dataset, the best fitting parameter from this search was comparable with the parameters generalized from the training dataset ( $R^2$ : 0.77 [0.71, 0.95],  $RMSE$ : 142.69 [107.82, 211.02]). Moreover, performance across the 162 parameter settings was relatively stable, yielding a moderate range of R-squared ( $M = 0.62$ ;  $SD = 0.1$ ) and  $RMSE$  ( $M = 181.75$ ;  $SD = 23.28$ ). Finally, the qualitative ordering of the dishabituation magnitude was also preserved when averaged across all parameter settings.

### Comparison with alternative models

To examine whether the three components — the perceptual representation, the learning model, and the decision model — in our models were critical to the success of our model, we ran three alternative models: Random Embedding model, No Noise model, and No Learning Model. We ran a parameter search for each of the model, and all of the models showed worse performance compared to RANCH (Random Embedding:  $R^2$ : 0.57 [0.08, 0.89],  $RMSE$ : 195.06 [147.39, 288.47]; No Noise:  $R^2$ : 0.45 [0.34, 0.85],  $RMSE$ : 221.46 [167.34, 327.5]; No Learning:  $R^2$ : 0.28 [0.19, 0.76],  $RMSE$ : 253.46 [191.52, 374.83]).

### Discussion

In this paper, we report on a novel experiment in which participants are familiarized to sequences of animations, and we measure habituation and their dishabituation to different

types of violations of familiar stimuli. We find that adults’ dishabituation is graded by the type of violation they see, and that the magnitude of dishabituation is predicted by a rational model which takes noisy samples from perceptual embeddings of the same stimuli that participants saw. Our model, RANCH, through its use of perceptual embeddings, operates directly on raw images and therefore can generate predictions for previously unseen stimuli or even tasks. Making use of this property, we tested RANCH’s performance on our graded dishabituation task using parameters fit to behavior on a completely different self-paced looking time task.

Lesioning RANCH by removing key components caused its fit to the data to drop substantially relative to the full model and eliminated any sense of qualitative correspondence to the human data. This result suggests that the aspects that we lesioned - a psychologically-plausible embedding space, noisy perception, connecting sampling to concept learning - are all essential for explaining behavior in our task.

There are several directions in which RANCH could be extended in future work. First, in the current paper, we implemented a specific version of RANCH, with a specific form for each of its components: the perceptual representation, the learning model, and the linking hypothesis between learning and attentional sampling. However, RANCH’s modular and interpretable structure allows researchers to adjust its components according to the population or task for which predictions are being generated. For example, the perceptual embedding space used in this paper was aligned to adult behav-

ior (Lee, 2022), but infants likely represent visual objects differently from adults. Using perceptual representations based on visual input experienced by infants may provide a better fit to infant data (Orhan & Lake, 2023; Zhuang et al., 2021). Similarly, task settings in which there was hierarchical structure to the stimuli sequences would call for more complicated learning models. The linking hypothesis can also vary: In previous work we have also explored the effect of replacing the rational, but computationally expensive, EIG with easier-to-compute information-theoretic quantities such as surprisal or KL-divergence (Cao et al., 2023; Raz et al., 2023). While previous work has found that these linking hypotheses are interchangeable in the current context, it is possible that they would dissociate under different task settings or different assumptions about the perceptual representations.

Second, while inspired by infant looking time research, our current work only has adult participants. Beyond encoding stimuli differently from infants, adults may conceptualize our task differently from infants, and experience different task demands. In particular, infants are quite sensitive to changes in the number of objects that are displayed (Feigenson & Carey, 2003; Wynn, 1992), but in the current study, adults dishabituated to number violations as little as to pose violations, the subtlest violation in our task. This suggests that adults may have not engaged their number cognition in the way we would expect infants to in this task. Furthermore, given the interpretability of the model parameters we fit to behavior, conducting the same experiment with infants may lead to interpretable developmental differences in the model parameters, such as priors on perceptual noise and prior uncertainty about the mean and standard deviation of perceptual concepts.

Overall, our work presents a rational model, RANCH, which describes how humans decide how long to look at stimuli. Using a psychologically motivated visual encoding model allows RANCH to operate on raw images, and generate predictions for previously unseen stimuli or tasks. We think that the generality and interpretability of our model framework constitutes a significant step towards predictive modeling of adult, and eventually infant, looking time, thereby putting the field on firmer ground.

## References

- 10 Anderson, J. R. (1991). Is human cognition adaptive? *Behavioral and Brain Sciences*, 14(3), 471–485.
- Aslin, R. N. (2007). What’s in a look? *Developmental Science*, 10(1), 48–53.
- Baillargeon, R., Spelke, E. S., & Wasserman, S. (1985). Object permanence in five-month-old infants. *Cognition*, 20(3), 191–208.
- Blumberg, M. S., & Adolph, K. E. (2023). Protracted development of motor cortex constrains rich interpretations of infant cognition. *Trends in Cognitive Sciences*.
- Cao, A., Raz, G., Saxe, R., & Frank, M. C. (2023). Habituation reflects optimal exploration over noisy perceptual samples. *Topics in Cognitive Science*, 15(2), 290–302.
- Doshi, F. R., & Konkle, T. (2023). Cortical topographic motifs emerge in a self-organized map of object space. *Science Advances*, 9(25), eade8187.
- Dubey, R., & Griffiths, T. L. (2020). Reconciling novelty and complexity through a rational analysis of curiosity. *Psychological Review*, 127(3), 455.
- Fantz, R. L. (1963). Pattern vision in newborn infants. *Science*, 140(3564), 296–297.
- Feigenson, L., & Carey, S. (2003). Tracking individuals via object-files: Evidence from infants’ manual search. *Developmental Science*, 6(5), 568–584.
- Haith, M. M. (1980). *Rules that babies look by: The organization of newborn visual activity*. Lawrence Erlbaum Associates.
- Haith, M. M. (1998). Who put the cog in infant cognition? Is rich interpretation too costly? *Infant Behavior and Development*, 21(2), 167–179.
- Hebart, M. N., Zheng, C. Y., Pereira, F., & Baker, C. I. (2020). Revealing the multidimensional mental representations of natural objects underlying human similarity judgements. *Nature Human Behaviour*, 4(11), 1173–1185.
- Hunter, M. A., & Ames, E. W. (1988). A multifactor model of infant preferences for novel and familiar stimuli. *Advances in Infancy Research*.
- Kidd, C., Piantadosi, S. T., & Aslin, R. N. (2012). The goldilocks effect: Human infants allocate attention to visual sequences that are neither too simple nor too complex. *PloS One*, 7(5), e36399.
- Lee, M. J. (2022). *Rapid visual object learning in humans is explainable by low-dimensional image representations* (PhD thesis). Massachusetts Institute of Technology.
- Lieder, F., & Griffiths, T. L. (2020). Resource-rational analysis: Understanding human cognition as the optimal use of limited computational resources. *Behavioral and Brain Sciences*, 43, e1.
- Oaksford, M., & Chater, N. (1994). A rational analysis of the selection task as optimal data selection. *Psychological Review*, 101(4), 608.
- Orhan, A. E., & Lake, B. M. (2023). What can generic neural networks learn from a child’s visual experience? *arXiv Preprint arXiv:2305.15372*.
- Paulus, M. (2022). Should infant psychology rely on the violation-of-expectation method? Not anymore. *Infant and Child Development*, 31(1), e2306.
- Poli, Francesco, Ghilardi, T., Mars, R. B., Hinne, M., & Hunnius, S. (2023). Eight-month-old infants meta-learn by downweighting irrelevant evidence. *Open Mind*, 7, 141–155.
- Poli, F., Serino, G., Mars, R., & Hunnius, S. (2020). Infants tailor their attention to maximize learning. *Science Advances*, 6(39), eabb5053.
- Raz, G., Cao, A., Saxe, R., & Frank, M. (2023). Modeling habituation in infants and adults using rational curiosity over perceptual embeddings. In *Intrinsically-motivated and open-ended learning workshop@ NeurIPS2023*.

- Raz, G., & Saxe, R. (2020). Learning in infancy is active, endogenously motivated, and depends on the prefrontal cortices. *Annual Review of Developmental Psychology*, 2, 247–268.
- Schrimpf, M., Kubilius, J., Lee, M. J., Murty, N. A. R., Ajemian, R., & DiCarlo, J. J. (2020). Integrative benchmarking to advance neurally mechanistic models of human intelligence. *Neuron*, 108(3), 413–423.
- Wynn, K. (1992). Addition and subtraction by human infants. *Nature*, 358(6389), 749–750.
- Yamins, D. L., Hong, H., Cadieu, C. F., Solomon, E. A., Seibert, D., & DiCarlo, J. J. (2014). Performance-optimized hierarchical models predict neural responses in higher visual cortex. *Proceedings of the National Academy of Sciences*, 111(23), 8619–8624.
- Zhuang, C., Yan, S., Nayebi, A., Schrimpf, M., Frank, M. C., DiCarlo, J. J., & Yamins, D. L. (2021). Unsupervised neural network models of the ventral visual stream. *Proceedings of the National Academy of Sciences*, 118(3), e2014196118.